THE JOURNAL OF BIOLOGICAL CHEMISTRY
Vol. 276, No. 9, Issue of March 2, pp. 6779–6788, 2001

Printed in U.S.A.

Structural Transformations Accompanying the Assembly of Bacteriophage P22 Portal Protein Rings *in Vitro**

Received for publication, August 23, 2000, and in revised form, November 16, 2000
Published, JBC Papers in Press, November 22, 2000, DOI 10.1074/jbc.M007702200

Sean D. Moore‡ and Peter E. Prevelige, Jr.§

From the Department of Microbiology, University of Alabama at Birmingham, Birmingham, Alabama 35294

The *Salmonella typhimurium* bacteriophage P22 assembles an icosahedral capsid precursor called a procapsid. The oligomeric portal protein ring, located at one vertex, comprises the conduit for DNA entry and exit. In conjunction with the DNA packaging enzymes, the portal ring is an integral component of a nanoscale machine that pumps DNA into the phage head. Although the portal vertex is assembled with high fidelity, the mechanism by which a single portal complex is incorporated during procapsid assembly remains unknown. The assembly of bacteriophage P22 portal rings has been characterized *in vitro* using a recombinant, His-tagged protein. Although the portal protein remained primarily unassembled within the cell, once purified, the highly soluble monomer assembled into rings at room temperature at high concentrations with a half time of approximately 1 h. Circular dichroic analysis of the monomers and rings indicated that the protein gained α-helicity upon polymerization. Thermal denaturation studies suggested that the rings contained an ordered domain that was not present in the unassembled monomer. A combination of 4,4′-dianilino-1,1′-binapthyl-5,5′-disulfonic acid (bis-ANS) binding fluorescence studies and limited proteolysis revealed that the N-terminal portion of the unassembled subunit is metastable and is susceptible to structural perturbation by bis-ANS. In conjunction with previously obtained data on the behavior of the P22 portal protein, we propose an assembly model for P22 portal rings that involves a meta-stable monomeric subunit.

The capsid proteins of many viruses are capable of self-assembling into icosahedral structures with remarkable symmetry and fidelity. During the morphogenesis of the double-strand DNA-containing phage, the icosahedral symmetry of the head is interrupted by the presence of a unique portal vertex. In all double-strand DNA phage characterized thus far, this vertex is occupied by a single protein arranged as an oligomeric ring (1–3). In each case, the portal rings have symmetries that differ from the symmetry of the surrounding capsid resulting in a symmetry mismatch that precludes a regular interaction between the portal and capsid proteins (1). It has been suggested that this symmetry mismatch allows for portal rotation during DNA packaging (1). The formation of this vertex is essential for viability, because it comprises a conduit through which the DNA enters and leaves the head during the viral life cycle. Assembly intermediates during head formation are short-lived and have not been characterized. This has hampered efforts to characterize the mechanism of portal vertex formation. The well-characterized assembly pathway of bacteriophage P22 is ideally suited for the continued investigation of such interactions.

During bacteriophage P22 morphogenesis, the earliest detectable assembly intermediate is a procapsid (4, 5), which is composed of a T = 7 icosahedral shell of coat protein surrounding a scaffolding protein core (6), and ~12 molecules of the 84-kDa gene *1*-encoded portal protein (7, 8). These three proteins (portal, coat, and scaffolding) are the only structural gene products required for head assembly and DNA packaging (9, 10). An enzyme complex called a terminase binds to the portal vertex, and together, this DNA translocation machine pumps the concatameric viral DNA into the procapsid in an ATP-dependent manner (11–13). After the head has been filled, the terminase complex cleaves the DNA releasing the mature head (12). Mutants in the portal proteins of bacteriophages SPP1 and P22 have been isolated that alter the packing density of the DNA, suggesting that portal rings are part of the gauge regulating packaging (14–16). Following packaging, the proteins of the tail machine assemble at the portal vertex, stabilize the mature head, and result in an infectious virion (17).

The ability of portal protein to form oligomeric rings without head assembly has been reported for a number portal proteins studied thus far, including those of phages T4, φ29, Lambda, T3, and SPP1 (18–22). Likewise, purified wild-type P22 portal protein spontaneously formed rings with 12-fold rotational symmetry upon storage (8). Portal rings represent a class of structures capable of fully surrounding DNA in a nonspecific manner, analogous to the ring-like sliding clamps that have been recognized as integral components of DNA replication machinery (23, 24). A distinguishing feature of sliding clamps is that they are topologically closed in their functional state and so, in the absence of DNA threading, they must be assembled in place around the DNA (23, 24). Little is known regarding the mechanism by which the transformation from unassembled subunits to functional rings occurs. In this manuscript we report a more detailed characterization of the polymerization of P22 portal protein and provide insight into a potential control mechanism for ring assembly.

EXPERIMENTAL PROCEDURES

Cloning a His-tagged Portal—Bacteriophage P22 gene *1* (portal) was amplified by PCR[1] from a wild-type phage stock (c1 (25)). The amplified product was digested at primer-encoded restriction sites, ligated into

* This work was supported in part by National Institutes of Health (NIH) Grant GM47980. The costs of publication of this article were defrayed in part by the payment of page charges. This article must therefore be hereby marked "*advertisement*" in accordance with 18 U.S.C. Section 1734 solely to indicate this fact.

‡ Supported by an NIH Basic Mechanisms in Virology pre-doctoral fellowship.

§ To whom correspondence should be addressed: Dept. of Microbiology, University of Alabama at Birmingham, BBRB Rm. 416, 845 South 19th St., Birmingham, AL 35205. Tel.: 205-975-5339; Fax: 205-975-5479; E-mail: prevelig@uab.edu.

[1] The abbreviations used are: PCR, polymerase chain reaction; PAGE, polyacrylamide gel electrophoresis; SEC, size exclusion chroma-

the pET-21b plasmid (Novagen, Madison, WI), and transformed into *Escherichia coli* BL-21 (Novagen) for expression. DNA sequencing was used to verify that the recombinant portal gene contained the wild-type portal coding sequence with a C-terminal addition of a Leu-Glu linker (resulting from an *Xho*I site) and six consecutive histidines.

Construction of a Phage with His-tagged Portal—A P22 phage strain carrying the C-terminal His_6-tagged portal protein was generated by recombination. To allow for the efficient double-crossover needed to rescue a lethal point mutation in the phage genome, the recombination template plasmid contained the C-terminal His-tag sequence flanked on either side by ~1000 base pairs of DNA complementary to the phage genome flanking the gene *1*/gene *8* junction. The template was made by ligating two PCR products that had been digested with *Ase*I (primer-encoded, on the right and left ends respectively): One contained approximately the last 1000 base pairs of the His-tagged portal gene and was generated from the expression plasmid described above, the other contained ~1000 base pairs to the right of gene *1* and was generated from a wild-type phage stock. The ligated template was gel-purified and ligated into the pCR-Blunt plasmid (Invitrogen, Carlsbad, CA). To maintain the stop codon found in the wild-type portal gene, a TAA codon was introduced in place of the TGA codon found on the portal expression plasmid. In addition, the *Ase*I site used for ligating the recombination template remained in the recombinant virus genome immediately after the gene *1* stop codon altering the wild-type gene *1*/gene *8* junction.

This recombination plasmid was electroporated into *Salmonella typhimurium* strain DB7000 (26) as previously described (27). Phage containing a cold-sensitive point mutation in the 5′ region of the portal gene (1^{-}*cs*H137 13^{-}*am*H101 (26)) were grown on DB7000 containing the recombination template at restrictive temperature. Plaques from the template-rescued population were screened by immunoblotting with a commercial antibody that recognized four consecutive histidines (Qiagen, Valencia, CA). Phage that gave rise to positive immunoblots were prepared as phage stocks, and the gene *1*/gene *8* junction was sequenced to verify the presence of the His-tag in gene *1*.

Purified phage containing the his-tagged portal were analyzed by SDS-PAGE to determine the stoichiometries of the phage proteins and compared with those of wild-type phage. No differences were detected. The portal protein band in the purified phage was full-length and was recognized by an anti-His-tag antibody. These phage were then examined by negative-stain electron microscopy and found to be indistinguishable from wild-type P22.

Protein Expression and Purification—To generate soluble protein, 500 ml of the expression host was grown at 37 °C under ampicillin selection in 2× LB broth to an A_{600} of 0.7, induced with 1 mM isopropyl-1-thio-β-D-galactopyranoside, and shifted to 28 °C for 5–6 h. The cells were then harvested by centrifugation, resuspended in 1/20 volume of cold nickel binding buffer (20 mM imidazole, 20 mM Tris-Cl, 500 mM NaCl, pH 7.9) containing 0.2 mg/ml chicken egg white lysozyme, and frozen at −70 °C. Induction levels were estimated by SDS-PAGE and found to be ~300 mg of portal protein per liter of cells.

The cells were thawed at room temperature and two protease inhibitor tablets were added (EDTA-free Mini Protease Inhibitor mixture, Roche Molecular Biochemicals, Indianapolis, IN); the suspension was placed on ice, allowed to lyse, sonicated to reduce viscosity, and centrifuged to pellet material >~1000 S. Portal protein was isolated at 4 °C from 25 ml of lysate by binding to a 5-ml nickel column (HiTrap chelating, Amersham Pharmacia Biotech, Piscataway, NJ), washing with ~40 ml of 65 mM imidazole (in binding buffer), and eluting with ~10 ml of 500 mM imidazole (in binding buffer). Portal protein stored in the elution buffer precipitated, and EDTA was needed to maintain solubility at this step; therefore, the protein was eluted into a tube containing enough 200 mM EDTA such that the final EDTA concentration was ~10 mM. The portal protein was usually contained in a 10- to 15-ml elution volume at a concentration of 8–10 mg/ml. The entire process from thawing to elution from the nickel column was usually accomplished within 2 h.

Further purification was performed using anion-exchange and size-exclusion chromatography (see "Results"). For long-term storage, purified monomer was diluted to ~0.5 mg/ml and frozen in aliquots at −70 °C. Freezing and thawing the protein under these conditions did not cause detectable aggregation nor did it cause polymerization. The total yield of pure monomer was generally ~60 mg per 500-ml culture determined spectrophotometrically in 6.0 M guanidine-HCl using a calculated extinction coefficient of 99,740 M^{-1} cm^{-1} (28).

Purified, recombinant portal protein was recognized by polyclonal antibodies against wild-type portal protein, and also by anti-His_4 antibodies (Qiagen). The purified monomeric portal protein was analyzed using matrix-assisted laser desorption time of flight mass spectroscopy to verify the molecular mass (83.6 kDa), and the integrity of the N- and C termini were verified by tryptic and cyanogen bromide cleavage followed by mass spectroscopic identification of the expected fragments (UAB Mass Spectroscopy Core Facility).

For use, the monomers were thawed on ice and concentrated (Macrosep 30, Pall Gelman Laboratory, Ann Arbor, MI followed by Centricon 30, Millipore, Bedford, MA) at 4 °C to minimize oligomerization. The concentrated sample was injected onto a size-exclusion column (tandem TSK6000/SW300), and the monomer peak was isolated into a tube sitting in ice. Rings were prepared by allowing a sample of concentrated monomer (50–100 mg/ml) to stand for 12–18 h at room temperature (~23 °C). The protein was then diluted to ~1 mg/ml and allowed to stand on ice for several hours. The ice equilibration step was essential for preparing a stable homogeneous ring population, because it apparently allowed time for unstable intermediates to dissociate to the point that they were biochemically distinct from intact rings. The rings were then purified using anion-exchange chromatography (see "Results"), concentrated, and collected from the ring peak after separation on a size-exclusion column.

Size-exclusion Chromatography—For protein preparation, portal monomer and rings were resolved using tandem TSK6000 PW_{XL} (Toso-Haas, Montgomeryville, PA) and 300SW (Waters, Milford, MA) analytical size-exclusion columns running in 100 mM NaCl, 50 mM Tris-Cl, 2 mM EDTA pH 7.4 at room temperature. For the kinetics experiments, the populations were separated with only a 300SW to reduce run time. Data were collected using the HPLC Manager program (Amersham Pharmacia Biotech) running on a PC. Chromatogram baselines were adjusted using the spectral analysis software Grams32 (Galactic Industries Corp., Salem, NH) and finally plotted using Origin 6.0 (Microcal, Northampton, MA).

Analytical Ultracentrifugation—Equilibrium sedimentation was performed using an XL-A analytical ultracentrifuge (Beckman Coulter, Fullerton, CA). Data were collected at 11,000, 13,000, and 15,000 rpm at 1.2, 0.9, and 0.6 mg/ml at 4 °C. A partial specific volume of 0.7288 for the portal protein was calculated from the primary amino acid sequence using the protein analysis software SedNTerp (University of New Hampshire, Durham, NH). The resulting concentration profiles were fit with the program Origin 4.1 (Microcal) utilizing the Beckman XL-A AutoR1 macro (Beckman Coulter), which allowed global fitting of the absorbance profiles. The resulting data was then exported and plotted using Origin 6.0 (Microcal).

Electron Microscopy—Phage or portal rings were diluted to ~0.05 mg/ml, adhered to a carbon-coated Formvar layer supported on a copper grid, blotted to remove excess material, fixed for 1 min with 0.5% formaldehyde, and stained for 20 s with a 2% solution of uranyl acetate prepared in water. Images were collected on film with an electron microscope (Hitachi Instruments, San Jose, CA) operating with an accelerating voltage 75 kV.

Determination of the Activation Energy of Ring Formation—Portal monomer was concentrated at 4 °C using a Centricon-30 (Millipore), the buffer was changed to 100 mM NaCl, 50 mM $NaHPO_4$, pH 7.4, using a spin column (Micro Bio-Spin 6, Bio-Rad, Hercules, CA), and aliquoted into thin-walled PCR tubes sitting on ice. To initiate polymerization, a sample was placed in the preheated block of a thermal cycle machine and incubated. At various times after the start of incubation, an aliquot from the tube was sufficiently diluted in HPLC buffer to stop ring formation (0.1 mg/ml), and the sample was analyzed using SEC (SW300).

The chromatographic peak of the rings overlapped that of intermediates, which prevented a baseline separation of the ring peak for integration. Therefore, to determine the contribution of rings to each chromatogram, each chromatogram was computationally deconvolved using singular value decomposition (SVD, (29, 30)). This was performed using an add-on array-BASIC SVD program running in Grams32 as previously described (31). The concentration of subunits in rings was determined by calculating the relative fractional contribution of a homogeneous ring chromatogram to each experimental chromatogram and then multiplying by the total concentration of protein present in each sample. These values were plotted *versus* time and fit to obtain relaxation times (τ) using the equation $y = y_0 + Ae^{-x/\tau}$ using Origin 6.0 (Microcal). The logarithms of the rate constants ($1/\tau$) from each fitted temperature series were plotted against reciprocal temperature to generate an Arrhenius plot, and a straight line was fitted to obtain the

tography; SVD, singular value decomposition; CD, circular dichroism, bis-ANS, 4,4′-dianilino-1,1′-binapthyl-5,5′-disulfonic acid.

slope of the data. The activation energy was obtained by calculating the negative of that slope by virtue of the Arrhenius relationship: $\ln k = -E_a/RT + C$ (32), where k is the rate constant, E_a is the apparent activation energy, R is the gas constant, T is the temperature, and C is a constant.

Circular Dichroism—The CD spectra were collected using an Aviv 62DS circular dichroism spectrophotometer (Aviv Instruments Inc., Lakewood, NJ). Far UV spectra from 200 to 260 nm were collected at a protein concentration of 0.2 mg/ml in phosphate buffer (100 mM NaCl, 50 mM $NaHPO_4$, pH 7.4) in a 0.1-cm path length cuvette at 25 °C. Data were collected at 0.5-nm intervals as the average of five scans with 10-s averaging at each wavelength. Under these conditions, high solvent absorbance prevented the collection of data below 200 nm.

Data were averaged and smoothed using the on-board software, the solvent background was subtracted, and the spectra were transferred to a separate PC for further analysis. The amount of secondary structure was estimated using the software program CDNN (version 2.1) (33). This program used a trained neural net algorithm to compare the experimental spectrum to a set of 33 reference spectra for which the secondary structure content is known. The reliability of the estimations of secondary structure content was determined by the closeness of the sum of percentages to 100%.[2]

Thermal denaturation of the monomers and rings were performed in a 1.0-cm path length stirred cuvette in phosphate buffer. The CD signal at 222 nm was collected in 0.5 °C steps with 20 s of averaging per step. Two independent melting plots were obtained using different preparations of monomer and ring. These were averaged to generate the plot in Fig. 6.

Bis-ANS Fluorescence Measurements—The fluorescent dye 4,4′-dianilino-1,1′-binapthyl-5,5′-disulfonic acid (bis-ANS, Molecular Probes, Eugene, OR) was prepared as a stock solution in 50% methanol, and the concentration was determined spectrophotometrically after dilution into water (ϵ_{385} = 16,790 M^{-1} cm^{-1}) (34). Fluorescence measurements were made with a Shimadzu RF-1501 fluorometer (Shimadzu Scientific, Columbia, MD) using λ_{ex} = 385 nm and λ_{em} = 485 nm. The fluorescence signal was corrected for background bis-ANS fluorescence and correcting for the inner-filter effect ($F_{corr} = F_{obs} \times 10(A_{385} + A_{485})/2]$) (35). Fluorescence measurements of bis-ANS and protein were made after allowing the mixed samples to equilibrate for 30 min prior to measurement. The fluorescence signal was stable for solutions of bis-ANS with monomers and rings.

Fitting of the reverse titration fluorescence data with the a single-site hyperbolic-binding function allowed determination of F_{max} which represented the signal of bis-ANS fully bound to the highest affinity site on the protein ($F_{obs} = (F_{max} \times L \times K_a)/(1 + L \times K_a)$), where F_{obs} equals the observed relative fluorescence signal above background, F_{max} is the maximum fluorescence signal of the ligand complex, L is the ligand concentration, and K_a is the apparent association constant (36). K_d ($1/K_a$) was then determined by calculating the free protein concentration during each measurement as a function of fluorescence and once again fitting with the same binding function (37).

Proteolytic Digestion—Portal monomers and rings were digested at 0.11 mg/ml with α-chymotrypsin (0.005 units/ml, Sigma Chemical Co., St. Louis, MO) at room temperature in 50 mM $NaHPO_4$, 100 mM NaCl, pH 7.4. At defined time points, aliquots were removed and placed into SDS sample buffer containing 2 mM phenylmethylsulfonyl fluoride and immediately heated to 100 °C for 5 min. These samples were then resolved using SDS-PAGE using a 12.5% gel and stained with Coomassie Blue.

RESULTS

His-tagged Portal Protein Functions in Vivo—Previous studies had indicated that the C-terminal 50 amino acids of the P22 portal protein are not required for phage viability (38, 39). Therefore, to obtain sufficient material for *in vitro* studies, and to simplify purification, a recombinant portal protein to which a poly-histidine tag was appended to the C terminus was constructed and overexpressed in *E. coli*. To verify that the His-tagged protein was functional, the gene for the His-tagged protein was crossed back into phage and the phage viability determined. Infectious phage utilizing the His-tag were recovered (designated P22 1His). The burst size of these phage was ~50% that of wild-type, indicating a slight effect of the presence of the His-tag portal gene on phage morphogenesis. The ability of phage 1His to plaque on P22-permissive *E. coli* (40) was also verified.

Portal Protein Oligomerizes upon Storage—Recombinant, His-tagged portal protein was overexpressed in *E. coli*, purified using nickel affinity chromatography, and analyzed by SDS-PAGE (Fig. 1*A*). The expressed protein was the dominant component of the lysate (Fig. 1*A*, *lane 2*), was retained on the nickel column, and eluted as an essentially pure protein at ~8 mg/ml (Fig. 1*A*, *lane 5*). A typical yield was 125 mg per 0.5 liter.

To determine the oligomerization state of the protein, an aliquot of the protein was diluted to 1 mg/ml and injected onto an SW300 size exclusion column (Fig. 1*B*). The sample eluted as two peaks: an included peak comprising ~80% of the protein, an excluded peak comprising ~10% of the protein. Species of intermediate sizes comprised the remaining 10%.

To determine the effect of concentration on polymerization, one aliquot of the purified protein was concentrated to 50 mg/ml, while another was maintained at 1 mg/ml. After 18 h of incubation at room temperature, the concentrated sample was diluted to 1 mg/ml, and both samples were analyzed by SEC (Fig. 1*B*). The protein that had not been concentrated still contained primarily the smaller, included form. In contrast, the sample that had been concentrated to 50 mg/ml displayed a shift toward higher molecular weight species, suggesting the existence of a concentration-dependent polymerization reaction.

The Small and Large Forms Can Be Isolated—To isolate the different forms of portal protein, the eluate from the nickel column was dialyzed against low salt buffer (50 mM Tris-Cl, 50 mM NaCl, 20 mM 2-mercaptoethanol, 2 mM EDTA, pH 7.4), centrifuged to remove large aggregates, loaded onto an anion exchange column, and eluted with an increasing gradient of NaCl (Fig. 2*A*). The protein resolved as a series of four dominant peaks eluting between 250 and 650 mM NaCl. Each peak was then examined by SEC (Fig. 2*B*). The protein that had eluted at the lowest salt concentration (*peak a*: 250–320 mM) eluted as a single peak that was fully included in the column matrix. The protein that had eluted at the highest salt concentration (*peak d*: 550–650 mM) eluted as a single peak that was fully excluded from the column matrix. Protein that had eluted at intermediate salt concentrations (*peaks b* and *c*) contained a mixture of both the small and large forms.

In a separate experiment, the stability of the different forms was determined. Samples from *peaks a*, *b*, and *d*, were incubated at either 4 or 23 °C overnight at 0.2 mg/ml. Samples from *peaks a* and *d* were unchanged, whereas the relative amount of small and large species in the sample from *peak b* displayed a temperature-dependent change in distribution. Low temperature favored the smaller form. Presumably this shift in distribution represented equilibration of long-lived intermediates to the stable final forms.

The Two Stable Portal Protein Forms Are Monomers and Rings—Wild-type portal protein was previously isolated from infected cells and characterized using SEC and rate-zonal sedimentation (8). From those data it was estimated that the unassembled form of the protein was either a monomer or a dimer. Similarly, the unassembled recombinant portal protein described here had an apparent molecular mass of 175 kDa, which was estimated by comparison of its SEC elution time to those of known standards (not shown). Although this was consistent with this form having been a dimer of the 84-kDa portal subunit, it was also possible that it represented an elongated monomer. Therefore, to obtain the shape-independent molecular mass of the small form of the protein, it was characterized using equilibrium analytical ultracentrifugation in the same

[2] G. Bohm, personal communication.

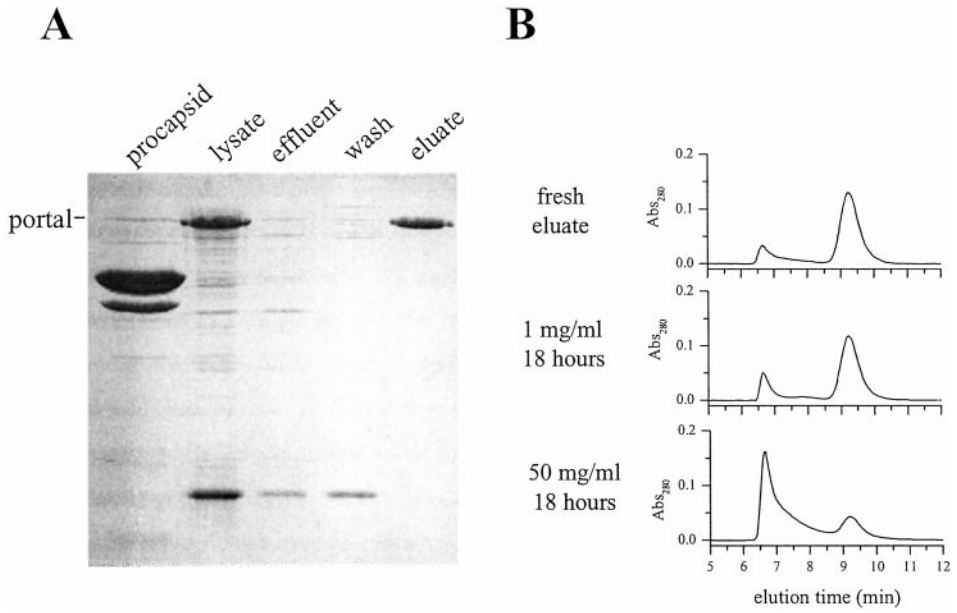

FIG. 1. **Purification of His-tagged portal protein analyzed by SDS-PAGE.** *A*, recombinant, His-tagged portal protein was overexpressed in *E. coli* and purified using nickel affinity chromatography. *Lanes*: *procapsid*, purified P22 procapsids that contained the 84-kDa portal protein; *lysate*, cleared bacterial lysate of induced expression host; *effluent*, lysate material that did not bind to the nickel column; *wash*, material removed with 65 mM imidazole; *eluate*, material eluted with 500 mM imidazole. Approximately 90% of the portal protein present in the lysate was recovered in the elution step. *B*, samples of purified portal protein were analyzed by SEC running in Tris buffer (100 mM NaCl, 50 mM Tris-Cl, 2 mM EDTA, pH 7.4). *Samples*: *fresh eluate*, a sample of protein immediately after elution from the nickel column after dilution in Tris buffer to 1.0 mg/ml; *1 mg/ml 18 h*, protein that was stored for 18 h at 1.0 mg/ml; *50 mg/ml 18 h*, protein that had been concentrated to 50 mg/ml for 18 h prior to dilution to 1 mg/ml for SEC analysis.

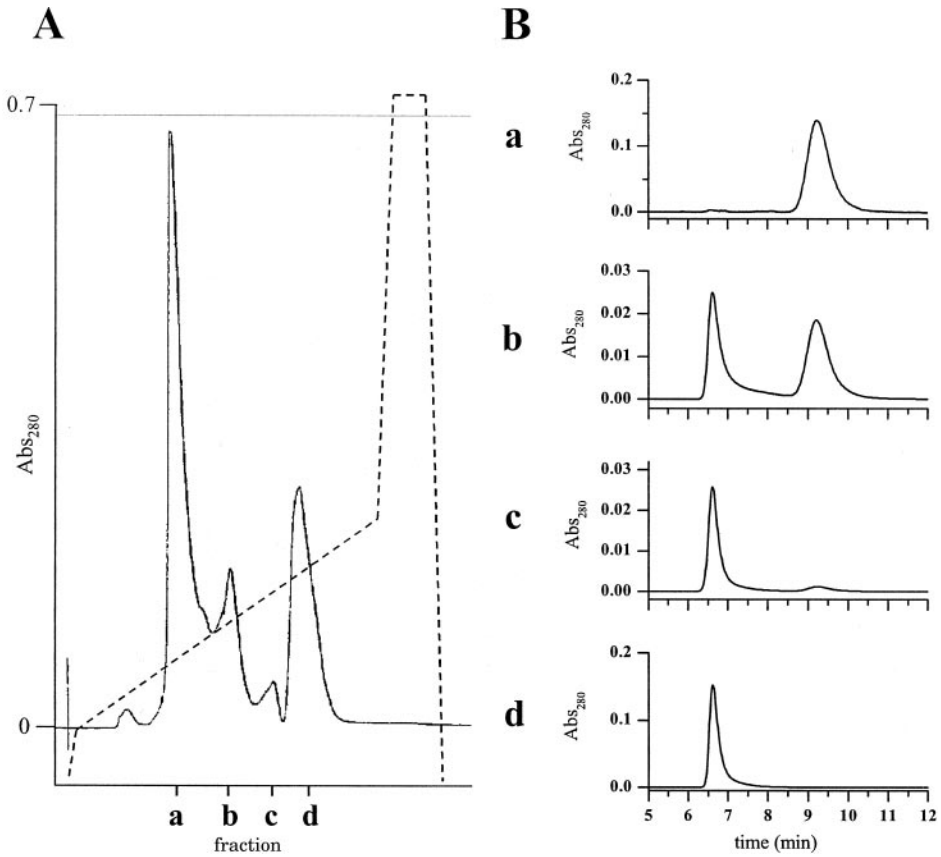

FIG. 2. **Isolation of monomers and rings.** *A*, purified portal protein in 100 mM NaCl was bound to an anion exchange column (Hi-Trap Q) and eluted with a NaCl gradient from 200 to 700 mM NaCl in Tris buffer at pH 7.4. All of the protein bound to the column and was eluted between 250 and 650 mM NaCl. The *dotted line* is the total gradient profile from 25 mM to 2 M NaCl. *B*, selected fractions from the anion exchange column characterized by SEC (SW300). *Lowercase letters a* through *d* correlate fractions from the ion exchange column with SEC chromatograms.

buffer used for the size exclusion chromatography (Fig. 3*A*). The best fit to a single species yielded a molecular mass of 87 kDa (± 4 kDa) with evenly distributed residuals. Attempts to fit the data with alternate multimeric protein models were unsuccessful. SEC analysis of the sample after the ultracentrifugation analysis verified that the protein had remained

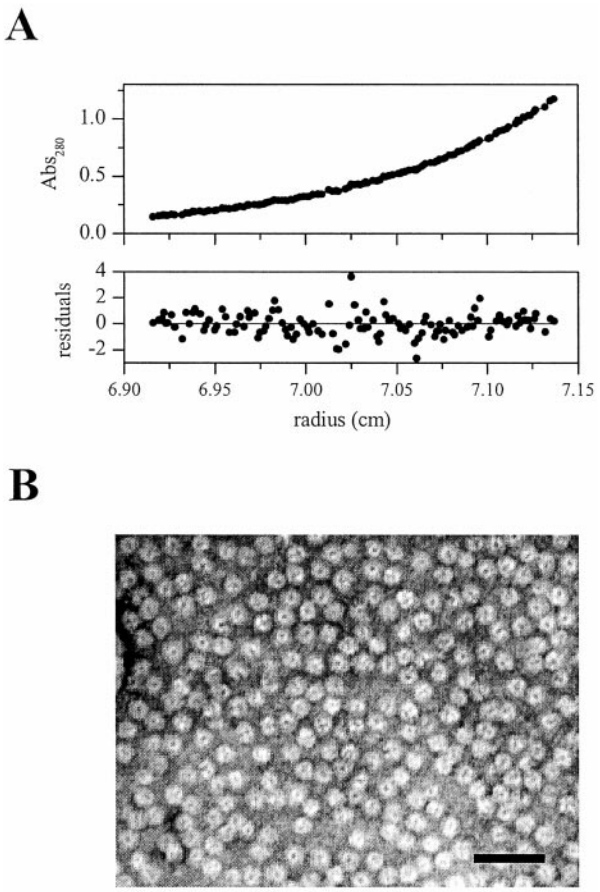

FIG. 3. **Assignment of the assembly state of the portal protein.** *A*, portal protein eluted with 320 mM NaCl from an anion exchange column was exchanged into Tris buffer (100 mM NaCl, 50 mM Tris-Cl, 2 mM EDTA, pH 7.4) and allowed to reach equilibrium in an analytical ultracentrifuge at three different concentrations at 4 °C. The equilibrium absorbance profiles were globally analyzed to obtain a molecular weight estimation. Shown here is the fit superimposed on representative absorbance data collected at 0.9 mg/ml. The residuals from this fit are plotted *below*. *B*, negative-stain electron micrograph of the portal protein eluted from the anion exchange column with 660 mM NaCl. The sample was stained with 2% uranyl acetate. The *scale bar* corresponds to 50 nm.

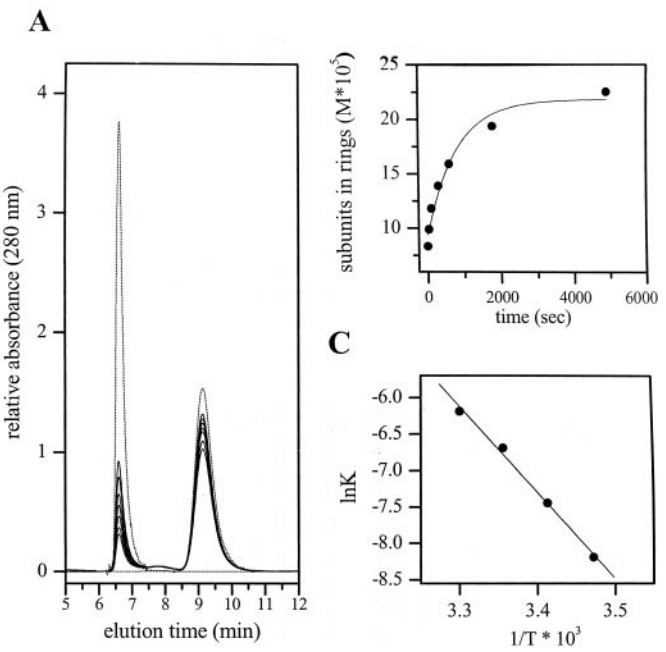

FIG. 4. **Ring assembly kinetics.** *A*, superimposed SEC chromatograms of portal protein at selected times after the commencement of assembly at 25 °C at 520 μM (44 mg/ml) in phosphate buffer. *Solid lines* are experimental chromatograms, and *dotted lines* are chromatograms of homogeneous monomer and ring used in the SVD-based quantification procedure. *B*, a plot of portal protein assembled as rings at various times at 25 °C. The data were fit using a single-exponential equation (*solid line*) to obtain a macroscopic forward rate constant. *C*, Arrhenius plot of rate constants from portal polymerizing at 15, 20, 25, and 30 °C. A *straight line* was fit to obtain the slope.

unassembled during the experiment. Therefore, the small form of the portal protein was an elongated monomer.

To determine the structure of the large form, a sample of protein that had been eluted from the anion exchange column with 650 mM NaCl was analyzed using negative-stain electron microscopy (Fig. 3*B*). The only visible structures were those of rings with outward-extending knobs. These structures were indistinguishable in size and morphology from rings that formed from wild-type protein (8), indicating that the large form of the protein was an oligomeric ring.

Portal Rings Assemble Slowly in Vitro—To better characterize the process of ring formation, the kinetics and thermodynamics of ring assembly were determined. The observation that the rings were stable once they had formed provided the opportunity to characterize their formation from monomeric portal subunits *in vitro*.

The polymerization of monomers into rings was greatly retarded at low temperatures; therefore, highly concentrated monomeric protein was stored on ice. Polymerization was triggered by rapidly raising the temperature by placing samples in a preheated block. Subsequently, aliquots were removed, diluted to 0.1 mg/ml to prevent further polymerization, and then analyzed using SEC (Fig. 4*A*). The amount of protein assembled as rings at each time point was quantified and plotted (Fig. 4*B*). The resulting data points were then fit using a single-exponential equation, and the apparent rate constant was determined from the best fit to the data. At a concentration of 44 mg/ml, only about half of the subunits was converted to rings after 1.5 h at 25 °C. The rate constants were similarly determined at 15, 20, and 30 °C, and an Arrhenius plot was then generated (Fig. 4*C*). The slope of such a plot equals the negative value of the activation energy. An activation energy of 12 kcal/mol of subunits was obtained.

Portal Protein Changes Secondary Structure—The conversion of monomer to rings required a high concentration of protein and was slow relative to the phage replication cycle (~45 min). This suggested that the protein required a structural change to polymerize. To determine whether there were changes in secondary structure when the portal protein formed rings, the far-UV circular dichroism spectra of purified monomer and rings were determined (Fig. 5). The CD spectra were collected at 25 °C at a concentration too low to promote ring formation during the measurements (0.2 mg/ml). The amount of monomer in the sample was determined before and after the CD measurement and determined to be ~96% in both cases. The rings used for this experiment were intact before and after the measurements as determined by SEC. The resultant CD spectra indicated that there was a considerable increase in secondary structure that accompanied ring formation. Both forms were highly α-helical as was evident by the spectral minima at 208 and 222 nm. To more accurately determine the secondary structural components within each form, each spectrum was analyzed using the program CDNN.

The monomeric portal protein was estimated to contain 41% α-helix, whereas the ring contained 49% α-helix. The increase

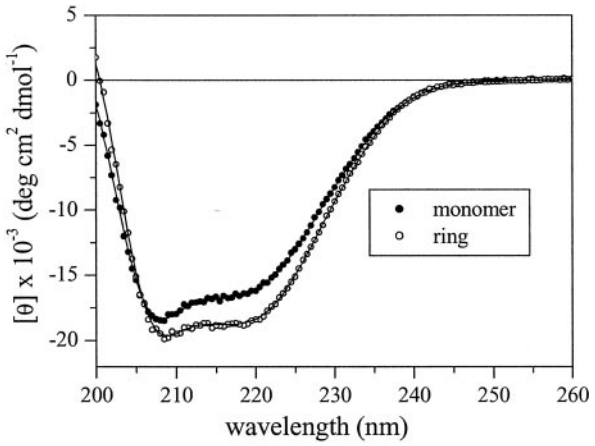

FIG. 5. **Far-UV CD spectra of the monomer and ring.** Averaged CD spectra of portal monomer (*filled circles*) and rings (*open circles*) from 200 to 260 nm at 25 °C in phosphate buffer (100 mM NaCl, 30 mM $NaHPO_4$, pH 7.4). The *straight lines* are the smoothed data generated for calculating the amount of secondary structure using the program CDNN. Monomer: 40.7% α-helix, 6.1% anti-parallel β-sheet, 4.8% parallel β-sheet, 18.7% β-turn, 27.9% random coil, Σ = 98.2%. Ring: 49.4% α-helix, 4.6% anti-parallel β-sheet, 4.9% parallel β-sheet, 15.9% β-turn, 25% random coil, Σ = 99.9%.

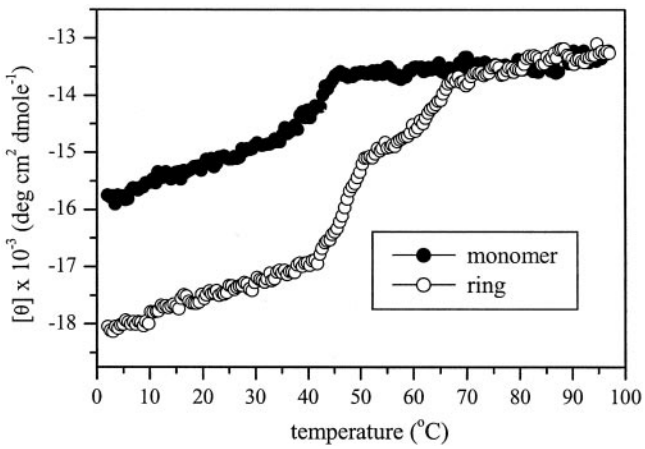

FIG. 6. **Thermal denaturation of the monomer and ring.** Portal monomer (*filled circles*) and ring (*open circles*) at 0.25 mg/ml were heated from 2 to 98 °C in phosphate buffer, and the CD signal at 222 nm was recorded. Each plot is the solvent-corrected average of two independently obtained melting profiles using different preparations of monomers and rings.

in α-helicity was accompanied primarily by a loss in random coil. Computational estimates of the absolute α-helical content of a protein are the most accurate and are generally within ~5% of the amount determined from high resolution structures (41). This error primarily arises from errors in the determination of protein concentration (33, 41) and from random noise (33). The CD spectra in Fig. 5 were averaged prior to smoothing to reduce noise error. The concentrations of monomers and rings, determined spectrophotometrically using denatured samples, were within 1% of each other. Therefore, the calculated changes in secondary structure upon ring formation are more accurate than the absolute calculations of secondary structure, probably with less than 3% error.

A New Domain Is Folded upon Ring Formation—The increase in α-helix corresponded to roughly 6–7 kDa of peptide ordering or ~60 amino acids (~8% of the 83.6-kDa subunit). Because this ordering involved a significant amount of the polypeptide backbone, it was possible that a new cooperative folding unit had been generated upon ring formation. To determine whether polymerization resulted in cooperative stabilization of the α-helical secondary structure within the subunit, both monomers and rings were thermally denatured, and the α-helical content of each was monitored by measuring the CD signal at 222 nm (Fig. 6). The monomeric protein exhibited a gradual loss of CD signal as the protein was heated from 2 to 37 °C. Between 37 and 45 °C, a single cooperative unfolding transition was observed that resulted in the loss of ~6% of the ellipticity at 222 nm. Once this transition had occurred, the CD signal remained constant up to 98 °C. The rings exhibited a gradual loss of CD signal from 2 to 43 °C. Two sharp melting transitions followed: one from 43 to 51 °C, and another from 55 to 68 °C. When combined, the amplitude of these two melting transitions accounted for the difference in CD signal at 222 nm that existed between the monomer and ring.

The thermal transition was irreversible for both forms. In addition, the CD spectra of the heated monomer and ring samples became super imposable after these melting transitions occurred. The spectra of the thermally denatured samples were different than either native spectrum. Using the CDNN software, the heat-denatured samples were estimated to contain ~31% α-helix at 25 °C. The loss of α-helicity from the native forms was accompanied by an increase in antiparallel β-sheet (to 10%) and random coil (to 31%). These structural changes were also accompanied by an increase in the turbidity of the samples and suggested that the protein had formed large aggregates upon heating.

To determine whether aggregation indeed accompanied heat denaturation, monomers and rings were heated to 30, 55, and 70 °C for 10 min and the products were then analyzed by SEC (tandem TSK6000/SW300). Monomers and rings both irreversibly aggregated above 55 °C, primarily to filterable aggregates (>0.1 μm). Because the changes in secondary structure that occurred upon heating the portal protein were irreversible, we did not evaluate the melting curves thermodynamically. The two cooperative transitions in the CD melting curve of the ring supported the observation that the subunit had gained α-helical secondary structure upon ring formation; however, using circular dichroism alone we could not determine which of the two cooperative domains present in the rings was also present in the monomers. Currently, we are characterizing the thermal and pressure stability of both forms by monitoring tryptophan fluorescence in an attempt to assign folded regions in the two forms.

Bis-ANS Binds to the Monomer and Ring—The *in vitro* polymerization experiments revealed that the polymerization into rings was greatly inhibited at low temperatures, suggesting a role for hydrophobic interactions in the assembly of rings (42). However, both monomers and rings were highly soluble at ambient temperatures, suggesting that large hydrophobic regions were not surface-exposed. To determine the nature of accessible hydrophobic regions of the monomer and ring, each form was probed with the fluorescent dye bis-ANS. This compound is a dimer of ANS and exhibits a very weak fluorescence in polar solvents due to solvent quenching (35, 43). The fluorescence of bis-ANS is greatly enhanced when the dye is bound within nonpolar cavities and has been used extensively to monitor accessible hydrophobic regions within proteins (37, 44–48).

Portal monomers and rings were incubated with increasing amounts of bis-ANS. The fluorescence signal was corrected for background fluorescence as well as the inner-filter effect (35) and plotted to represent the change in fluorescence as a function of bis-ANS concentration (Fig. 7). The observed fluorescence is a function of both the binding constant and the fluo-

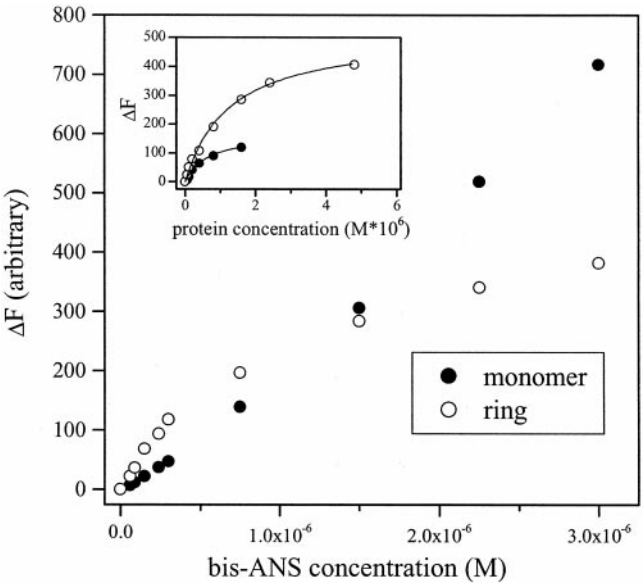

FIG. 7. **Bis-ANS binding fluorescence.** The relative fluorescence of bis-ANS was recorded in the presence of 80 nM portal protein either as monomers (*filled circles*) or assembled as rings (*open circles*) and plotted (ΔF). *Inset*, the fluorescence signal from 80 nM bis-ANS as it was titrated with increasing amounts or either monomer (*filled circles*) or rings (*open circles*). The *solid lines* superimposed on these plots are the best fits of the hyperbolic binding function that was used to obtain ΔF_{max}.

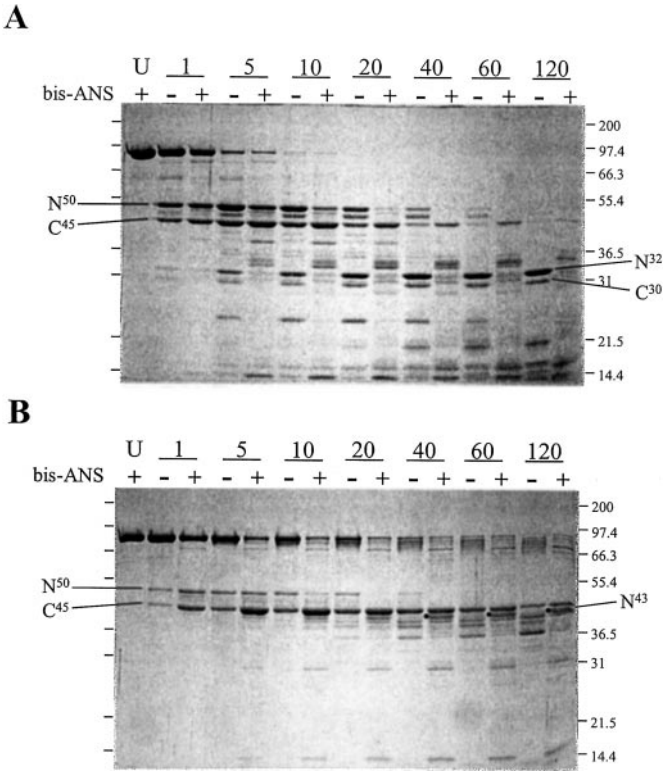

FIG. 8. **Proteolytic digestion in the presence of bis-ANS.** Portal protein (1.0 μM) was digested with α-chymotrypsin both with and without bis-ANS (100 μM) present. *A*, monomer digestion fragments; *B*, ring digestion fragments analyzed by SDS-PAGE. *Lane labels* indicate digestion time in minutes and whether or not bis-ANS was present. *N* and *C* denote fragments derived from the N- and C-terminal halves of the protein, respectively. *Superscripts* are approximate molecular masses in kilodaltons. The *black dots* in *B* denote fragment N^{43}. *Numbered tick marks* on the *sides* of each gel denote the positions and molecular masses in kilodaltons of standards (Mark-12, Novex, San Diego) run on a separate gel with selected digestion samples.

rescence enhancement accompanying binding (36, 49). At low concentrations of bis-ANS, the observed fluorescence was higher for the rings than for the monomers, whereas at high concentrations of bis-ANS this pattern was reversed. Significantly, the binding of bis-ANS to the rings approached saturation, whereas binding to the monomer did not (up to 2.25×10^{-5} M bis-ANS).

The nonsaturable binding behavior of the portal protein monomer is a result of having many weak binding sites (49) and has been observed in previous binding studies of bis-ANS and the chaperonin Cpn60 (50). Furthermore, the binding to the monomers was nonhyperbolic, suggesting that the binding of multiple bis-ANS molecules was altering the binding capacity of the subunit (36), presumably by inducing a structural change in the protein as has been reported for bis-ANS binding to other proteins (46, 51). The inability to saturate the monomers with bis-ANS prevented any determination of the total number of accessible binding sites, because the fluorescence emission per bis-ANS binding event could not be determined.

To minimize bis-ANS-induced structural perturbations, the binding to the portal protein was characterized in the presence of excess protein so that less than one bis-ANS molecule was bound per subunit (Fig. 7, *inset*). Under these conditions binding only occurs at the highest affinity sites (reviewed in Ref. 36). Fitting of these binding data with a hyperbolic binding function revealed that the bis-ANS bound the highest affinity site on the monomer with a K_d of 0.7 μM, whereas the high affinity binding to the ring had a K_d of 1.2 μM. In addition, the ring titration of bis-ANS gave the same binding isotherm as the bis-ANS titration of the rings, indicating that the rings bound only one bis-ANS molecule per subunit. The highest affinity binding site on the monomer had roughly twice the bis-ANS binding affinity of the rings. However, the lower fluorescence enhancement (Fig. 7, *inset*, lower F_{max}) of bis-ANS bound to this site suggested that it was more polar than the binding site on the rings. This argues that a substantial hydrophobic surface was not solvent-exposed on the monomer; yet, bis-ANS, when present at high molar excess, entered the less polar, hydrophobic regions of the monomer.

Polymerization Stabilizes the Portal Protein—The increase in α-helicity, coupled with the alterations in melting behavior and bis-ANS binding upon polymerization, suggested that ring assembly resulted in stabilization of a domain of the portal protein. To characterize stability changes that accompanied polymerization, both monomers and rings were subjected to partial proteolysis in the presence and absence of bis-ANS. The protein was digested at 23 °C, and samples removed at time points ranging from 0 to 120 min were treated with protease inhibitor and analyzed by SDS-PAGE. Fragments containing the C terminus were identified by performing Western blots using a monoclonal antibody that recognized the C-terminal His-tag (*bands* labeled C^x, where x is the approximate molecular mass in kilodaltons). To determine the origin of bands that did not contain the His-tag, fragments were excised and digested with trypsin, and the resultant peptides were identified by mass spectroscopy.

Fig. 8*A* shows the time course of digestion of portal monomers cleaved by α-chymotrypsin. An initial cleavage gave rise to two fragments of 45 and 50 kDa. These were derived from the C- and N-terminal regions of the protein, respectively (*bands* C^{45} and N^{50}). These two fragments were digested over the course of 120 min to yield fragments C^{30} and N^{32}. Tryptic peptides were obtained from fragment N^{32} corresponding to amino acids in the region spanning residues 15 to 145, thus

placing the origin of N^{32} at or very near the N terminus of the protein.

The subunits in the rings were more resistant to chymotrypsin cleavage than the monomers (Fig. 8*B*). After 5 min, the monomers had all been cleaved to smaller fragments, whereas intact ring subunits were detectable after 60 min. After 120 min of digestion, the ring subunits had been cleaved to a ladder ranging from ~70 to 90 kDa. The fragments C^{45} and N^{50} were also generated in the digestion of the rings; however, fragment C^{45} was generated more slowly. This suggests that the scissile bond connecting fragments C^{45} and N^{50} was more protected in the rings.

In the presence of bis-ANS, the rate of digestion of the monomers and rings was accelerated, indicating that bis-ANS was not inhibiting the enzyme. In addition to the enhanced digestion of the intact subunit, no detectable N-terminally derived fragments remained after 120 min of digestion of the monomer. During the digestion of the rings in the presence of bis-ANS, the cleavage that generated fragment C^{45} was enhanced. This suggests that the binding of bis-ANS was increasing accessibility to the scissile bond connecting C^{45} and N^{50}. In contrast to the digestion of the monomer, N-terminally derived fragments were present after 120 min of digestion in the presence of bis-ANS (*fragment* N^{43}, Fig. 8*B*). This presumably reflected a structural change in this region that had occurred as a result of polymerization.

The digestion experiments revealed that the portal protein was more resistant to proteolysis when assembled as rings, primarily at a scissile bond in the subunit that connected two large N- and C-terminal domains. Bis-ANS had apparently destabilized the N terminus of the monomer upon binding. Once assembled as rings, this region was more resistant to digestion in the presence of bis-ANS, suggesting that it had become more stable. The fluorescence analysis of bis-ANS binding, suggested that bis-ANS was denaturing a region of the monomer. Taken together, these data imply that the monomer contained a meta-stable domain that was stabilized upon ring formation.

DISCUSSION

Portal Protein Resists Polymerization—During the expression of the recombinant P22 portal protein, the intracellular concentration was estimated to be greater than 100 times that observed during a wild-type phage infection; however, the protein was recovered primarily as a monomer. Because the rings were stable in the buffers used for purification, we suspect that no dissociation occurred during purification and that the protein was primarily unassembled in the cell as well. The observation that portal protein rings did not readily assemble *in vivo* is in agreement with the previous finding by Bazinet and King (8) that unassembled P22 portal protein is isolated from infected *Salmonella* defective for coat protein production. The portal protein of bacteriophage SPP1, which has also been over expressed in *E. coli* and characterized *in vitro*, required divalent cations to form stable rings from monomeric subunits, and so it was suggested that the intracellular divalent cation concentration of the natural host (*Bacillus subtilis*) was sufficient to drive ring assembly (52). The P22 portal protein was expressed in a host that can support phage replication, suggesting that any requirements for ring assembly should have been met during expression. The finding that P22 portal protein rings did not appreciably form *in vivo* suggests that portal ring formation is tightly coupled to phage head assembly.

Once purified, the portal protein assembled into rings, albeit more slowly than required for phage morphogenesis. Kinetic measurements of the polymerization of the portal rings indicated that appreciable ring formation occurred only when the protein was highly concentrated. Even at high concentrations, the protein took hours to approach equilibrium implying that simple protein-protein collisions were not rate-limiting (53, 54). Slow protein oligomerization processes are generally limited by obligatory structural transformations that raise the activation energy of association (55). The observation that the P22 portal protein gained secondary structure upon polymerization suggests that this structural rearrangement is responsible for at least part of the observed 12 kcal/mol activation energy.

Protein Folding during Ring Formation—There was a pronounced structural change as the monomers became rings, primarily in the formation of α-helix. This is analogous to conformational changes that can accompany protein-protein and protein DNA associations (56, 57). Recent characterization of the P22 portal protein using Raman spectroscopy also revealed an increase in α-helical secondary structure upon polymerization, although the effect appeared to be less pronounced.[3] Recently, a high resolution structure of the ϕ29 connector (portal) was determined by x-ray crystallography and revealed substantial inter-subunit contacts between α-helical regions.[4] Although there is currently no high resolution structural information on the monomeric forms of any portal protein, it is not unreasonable to assume that additional secondary structure forms as a result of inter-subunit contacts.

The increase in secondary structure upon polymerization was accompanied by the formation of a cooperatively folded domain that was not present in the monomer. The folding of this domain may play a role in rendering the assembly process irreversible as in the case of some protein polymerization events (55, 58). It was determined that the monomer contained a meta-stable domain near the N terminus that was perturbed by bis-ANS binding. The monomers had the capacity to bind more bis-ANS than the rings, suggesting that the bis-ANS had access to hydrophobic regions within this domain that were inaccessible once the subunits had assembled. Indeed, some ring dissociation was observed after long incubations (>2 h) with excess bis-ANS, suggesting that bis-ANS was binding in regions that formed inter-subunit contacts (data not shown). An interesting aspect of the meta-stable domain in the monomer is that it was resistant to proteolytic digestion, suggesting that it contained a substantial amount of tertiary structure. This is supported by the observation that the tryptophan fluorescence of the monomer is blue-shifted relative to the ring, suggesting that this region is solvent-protected.[5] It is tempting to speculate that stabilization of this meta-stable domain is coupled to the observed folding increase.

A Meta-stable Monomer—Meta-stable proteins have been described as having little resistance to protease and are generally referred to as being molten-globule-like because of their lack of defined tertiary structure, similar to protein folding intermediates (57). It has been postulated that this property allows some proteins to adopt different conformations, because they bind to various regulatory factors allowing a wide range of specificity and function (56, 57). In addition, stabilizing the meta-stable regions in α-antitrypsin by directed mutagenesis impeded protein function, suggesting that escape from the meta-stable conformation can be coupled to biological activity (59).

Given that the P22 portal protein monomer is refractory to polymerization in the absence of phage head assembly, it is conceivable that the subunit utilizes a meta-stable domain to

[3] G. Thomas, personal communication.
[4] M. Rossman, personal communication.
[5] S. D. Moore and P. E. Prevelige, Jr., unpublished observation. The P22 portal protein contains 11 tryptophans, 10 of which are located in the N-terminal half of the protein.

refrain from premature ring formation. The observed activation barrier may be coupled to leaving this intermediate conformation prior to committing to the ring form. This mechanism could allow for strict temporal control of assembly within the cell, because initiation of ring assembly would require a "triggering" catalyst to lower the activation barrier for assembly: akin to the process of scaffold-catalyzed coat protein assembly observed in P22 (60) or the initiation of TMV coat assembly by RNA (61). Once initiated, autostery could then more efficiently recruit subunits to assemble into the growing ring (62, 63).

Why Control Ring Assembly?—Proteins destined to become members of multisubunit assemblies can fold into inactive forms to allow for kinetic control and pathway determination during assembly (63–65). Additionally, kinetic control can be an integral requirement for high fidelity assembly (66). Given that the P22 portal protein is capable of assembling into rings by itself, the presence of a kinetic barrier is intriguing. Perhaps preformed portal rings are detrimental to viral morphogenesis. We have recently determined that preassembled P22 portal rings are capable of stably binding to the P22 DNA packaging machinery (gp2 and gp3).[6] If this binding represents aberrant DNA packaging initiation, then the portal protein may be designed to prevent such catastrophic interactions by remaining unassembled until it is recruited into a growing head.

The reduced assembly rate may also reflect an evolutionary solution to an inherently difficult process: assembling the correct number of subunits into the portal rings. The intrinsic curvature of a growing ring may not be constrained sufficiently to ensure the production of only one symmetry with a defined number of subunits (67) (assuming that only one symmetry is utilized during viral morphogenesis). Indeed, it has been observed that the portal protein of bacteriophage T7 can assemble into rings with both 12- and 13-fold symmetry (68). Additionally, the 13-subunit portal ring of bacteriophage SPP1 assembles through intermediates with a curvature that correlates with a 14-subunit ring (22). Efficiently assembling portal rings with a defined number of subunits may require a scaffold to ensure the proper ring diameter. Thus, some portal proteins may be designed such that they only participate in assembly as members of an organizing complex. In the case of the portal protein of bacteriophage T4 the product of gene *40* serves this purpose (69). A model for portal vertex formation during bacteriophage T7 morphogenesis has been proposed that includes an interaction between the connector protein (p8) and the outer shell protein (p10A) at an early stage of head assembly (70). In this model, the connector assembles into a preformed hole in the capsid lattice. Such a mechanism hints that the capsid hole could be a guide for connector polymerization.

In the scheme of P22 head assembly, likely candidates for the role of portal activator are the scaffold and coat proteins, because they appear to be intimately involved in the assembly of the portal vertex. It has been proposed that phage-encoded RNA may also play a role in portal incorporation by serving as an organizing center (38). Mutants in the P22 scaffolding protein have been isolated that are unable to recruit portal protein into growing heads (71). Additionally, a mutant portal protein (*cs*H137), which is not recruited into procapsids under restrictive conditions, can be rescued by several different mutations in the P22 coat protein (26). This may reflect a general mechanism for portal incorporation, because physical interactions between scaffold, coat, and portal proteins have been observed for other phages (72, 73).

Acknowledgments—We thank those who assisted in the preparation of these experiments: Sherwood Casjens (University of Utah, Salt Lake), Jonathan King (Massachusetts Institute of Technology), and Miriam Susskind (University of Southern California), for generously providing both bacterial and phage strains; Peter Weigele (University of Utah, Salt Lake) for assistance in designing and synthesizing some of the PCR primers; and Grace Wu (University of Alabama) for her technical assistance.

[6] S. D. Moore and P. E. Prevelige, Jr., unpublished observation.

REFERENCES

1. Hendrix, R. W. (1978) *Proc. Natl. Acad. Sci. U. S. A.* **75,** 4779–4783
2. Hendrix, R. W. (1998) *Cell* **94,** 147–150
3. Valpuesta, J. M., and Carrascosa, J. L. (1994) *Q. Rev. Biophys.* **27,** 107–155
4. King, J., Lenk, E. V., and Botstein, D. (1973) *J. Mol. Biol.* **80,** 697–731
5. Lenk, E., Casjens, S., Weeks, J., and King, J. (1975) *Virology* **68,** 182–199
6. Casjens, S., and King, J. (1974) *J. Supramol. Struct.* **2,** 202–224
7. Botstein, D., and Levine, M. (1968) *J. Mol. Biol.* **34,** 643–654
8. Bazinet, C., Benbasat, J., King, J., Carazo, J. M., and Carrascosa, J. L. (1988) *Biochemistry* **27,** 1849–1856
9. Botstein, D., Waddell, C. H., and King, J. (1973) *J. Mol. Biol.* **80,** 669–695
10. Israel, V. (1977) *J. Virol.* **23,** 91–97
11. Jackson, E. N., Laski, F., and Andres, C. (1982) *J. Mol. Biol.* **154,** 551–563
12. Casjens, S., and Huang, W. M. (1982) *J. Mol. Biol.* **157,** 287–298
13. Poteete, A. R., Jarvik, V., and Botstein, D. (1979) *Virology* **95,** 550–564
14. Casjens, S., Wyckoff, E., Hayden, M., Sampson, L., Eppler, K., Randall, S., Moreno, E. T., and Serwer, P. (1992) *J. Mol. Biol.* **224,** 1055–1074
15. Tavares, P., Santos, M. A., Lurz, R., Morelli, G., de Lencastre, H., and Trautner, T. A. (1992) *J. Mol. Biol.* **225,** 81–92
16. Orlova, E. V., Dube, P., Beckmann, E., Zemlin, F., Lurz, R., Trautner, T. A., Tavares, P., and van Heel, M. (1999) *Nat. Struct. Biol.* **6,** 842–846
17. Strauss, H., and King, J. (1984) *J. Mol. Biol.* **172,** 523–543
18. Driedonks, R. A. (1981) *Prog. Clin. Biol. Res.* **64,** 315–323
19. Carrascosa, J. L., Vinuela, E., Garcia, N., and Santisteban, A. (1982) *J. Mol. Biol.* **154,** 311–324
20. Kochan, J., Carrascosa, J. L., and Murialdo, H. (1984) *J. Mol. Biol.* **174,** 433–447
21. Nakasu, S., Fujisawa, H., and Minagawa, T. (1985) *Virology* **143,** 422–434
22. van Heel, M., Orlova, E. V., Dube, P., and Tavares, P. (1996) *EMBO J.* **15,** 4785–4788
23. Waga, S., and Stillman, B. (1998) *Annu. Rev. Biochem.* **67,** 721–751
24. Tsurimoto, T. (1999) *Front Biosci.* **4,** D849–D858
25. Levine, M., and Schott, C. (1971) *J. Mol. Biol.* **62,** 53–64
26. Jarvik, J., and Botstein, D. (1975) *Proc. Natl. Acad. Sci. U. S. A.* **72,** 2738–2742
27. Casjens, S., Eppler, K., Sampson, L., Parr, R., and Wyckoff, E. (1991) *Genetics* **127,** 637–647
28. Gill, S. C., and von Hippel, P. H. (1989) *Anal. Biochem.* **182,** 319–326
29. Moonen, M. S., and De Moore, B. (1995) *SVD and Signal Processing, III*, Third Ed., Elsevier Science, New York, NY
30. van Holde, K. E., Johnson, W. C., and Ho, P. S. (1998) in *Principles of Physical Biochemistry* (van Holde, K. E., ed) pp. 438–447, Prentice-Hall, Inc., Upper Saddle River, NJ
31. Lanman, J., Tuma, R., and Prevelige, P. E., Jr. (1999) *Biochemistry* **38,** 14614–1423
32. Cantor, C. R., and Schimmel, P. R. (1980) *Biophysical Chemistry Part III: The Behaviour of Macromolecules*, pp. 1216–1219, W. H. Freeman and Company, San Francisco
33. Bohm, G., Muhr, R., and Jaenicke, R. (1992) *Protein Eng.* **5,** 191–195
34. Farris, F. J., W. G., Chiang, C. C., and Paul, I. C. (1978) *J. Am. Chem. Soc.* **100,** 4469–4474
35. Lakowicz, J. R. (1999) *Principles of Fluorescence Spectroscopy*, Second Ed., pp. 52–56, Plenum Publishing Corporation, London, UK
36. Eftink, M. R. (1997) *Methods Enzymol.* **278,** 221–257
37. Musci, G., Metz, G. D., Tsunematsu, H., and Berliner, L. J. (1985) *Biochemistry* **24,** 2034–2039
38. Bazinet, C., Villafane, R., and King, J. (1990) *J. Mol. Biol.* **216,** 701–716
39. Eppler, K., Wyckoff, E., Goates, J., Parr, R., and Casjens, S. (1991) *Virology* **183,** 519–538
40. Neal, B. L., Brown, P. K., and Reeves, P. R. (1993) *J. Bacteriol.* **175,** 7115–7118
41. Greenfield, N. J. (1996) *Anal. Biochem.* **235,** 1–10
42. Kauzmann, W. (1959) *Adv. Protein Chem.* **14,** 1–63
43. Stryer, L. (1965) *J. Mol. Biol.* **13,** 482–495
44. Brand, L., and Gohlke, J. R. (1972) *Annu. Rev. Biochem.* **41,** 843–868
45. Horowitz, P., Prasad, V., and Luduena, R. F. (1984) *J. Biol. Chem.* **259,** 14647–14650
46. Shi, L., Palleros, D. R., and Fink, A. L. (1994) *Biochemistry* **33,** 7536–7546
47. Smulders, R. H., and de Jong, W. W. (1997) *FEBS Lett.* **409,** 101–104
48. Gaspar, L. P., Johnson, J. E., Silva, J. L., and Da Poian, A. T. (1997) *J. Mol. Biol.* **273,** 456–466
49. Weber, G. (1975) *Adv. Protein Chem.* **29,** 1–83
50. Horowitz, P. M., Hua, S., and Gibbons, D. L. (1995) *J. Biol. Chem.* **270,** 1535–1542
51. Vanderheeren, G., Hanssens, I., Noyelle, K., Van Dael, H., and Joniau, M. (1998) *Biophys. J.* **75,** 2195–2204
52. Jekow, P., Behlke, J., Tichelaar, W., Lurz, R., Regalla, M., Hinrichs, W., and Tavares, P. (1999) *Eur. J. Biochem.* **264,** 724–735
53. Northrup, S. H., and Erickson, H. P. (1992) *Proc. Natl. Acad. Sci. U. S. A.* **89,** 3338–3342
54. Koren, R., and Hammes, G. G. (1976) *Biochemistry* **15,** 1165–1171
55. Jaenicke, R., and Lilie, H. (2000) in *Advances in Protein Chemistry: Protein Folding Mechanisms* (Matthews, C. R., ed) Vol. 53, pp. 329–401, Academic Press, San Diego
56. Spolar, R. S., and Record, M. T., Jr. (1994) *Science* **263,** 777–784

57. Wright, P. E., and Dyson, H. J. (1999) *J. Mol. Biol.* **293,** 321–331
58. Tuma, R., Prevelige, P. E., Jr., and Thomas, G. J., Jr. (1998) *Proc. Natl. Acad. Sci. U. S. A.* **95,** 9885–9890
59. Lee, C., Park, S. H., Lee, M. Y., and Yu, M. H. (2000) *Proc. Natl. Acad. Sci. U. S. A.* **97,** 7727–7731
60. Prevelige, P. E., Jr., Thomas, D., and King, J. (1988) *J. Mol. Biol.* **202,** 743–757
61. Caspar, D. L., and Namba, K. (1990) *Adv. Biophys.* **26,** 157–185
62. Asakura, S., Eguchi, G., and Iino, T. (1966) *J. Mol. Biol.* **16,** 302–316
63. Caspar, D. L. (1980) *Biophys. J.* **32,** 103–138
64. Asakura, S. (1968) *J. Mol. Biol.* **35,** 237–239
65. King, J. (1971) *J. Mol. Biol.* **58,** 693–709
66. Schwartz, R., Shor, P. W., Prevelige, P. E., Jr., and Berger, B. (1998) *Biophys. J.* **75,** 2626–2636
67. Moody, M. F. (1999) *J. Mol. Biol.* **293,** 401–433
68. Kocsis, E., Cerritelli, M. E., Trus, B. L., Cheng, N., and Steven, A. C. (1995) *Ultramicroscopy* **60,** 219–228
69. Michaud, G., Zachary, A., Rao, V. B., and Black, L. W. (1989) *J. Mol. Biol.* **209,** 667–681
70. Serwer, P. (1987) *J. Theor. Biol.* **127,** 155–161
71. Greene, B., and King, J. (1996) *Virology* **225,** 82–96
72. Droge, A., Santos, M. A., Stiege, A. C., Alonso, J. C., Lurz, R., Trautner, T. A., and Tavares, P. (2000) *J. Mol. Biol.* **296,** 117–132
73. Guo, P. X., Erickson, S., Xu, W., Olson, N., Baker, T. S., and Anderson, D. (1991) *Virology* **183,** 366–373